

# Pulsar Wind Nebulae and the Non-thermal X-Ray Emission of Millisecond Pulsars

K. S. Cheng<sup>1</sup>, Ronald E. Taam<sup>2</sup>, and W. Wang<sup>3</sup>

<sup>1</sup> Department of Physics, University of Hong Kong, Pokfulam Road, Hong Kong, China

<sup>2</sup> Northwestern University, Dept. of Physics & Astronomy, 2145 Sheridan Rd., Evanston, IL 60208, USA

<sup>3</sup> Max-Planck-Institut für extraterrestrische Physik, Postfach 1312, 85741 Garching, Germany

## ABSTRACT

The non-thermal, non-pulsed X-ray emission of MSPs is investigated. As in young pulsars, MSPs emit a relativistic wind, which interacting with the interstellar medium and/or a binary companion can significantly contribute to the non-pulsed emission of these pulsars. An application and extension of a simple model developed for young pulsars is applied to the old recycled MSP B1957+20. It is found that the pulsar wind can, indeed, contribute to both the resolved and unresolved X-ray emission. For other MSP in the Galactic field where the spectral index of the non-pulsed component has been measured (i.e., PSR B1937+21, J0218+4232) the contribution of the pulsar wind to the non-pulsed X-ray luminosity is estimated. For the MSPs in the core regions of globular clusters, the pulsar wind nebula is likely affected by its interaction with the dense stellar environment, possibly leading to a diminished contribution to the total X-ray emission. In this case, the existence of non-thermal non-pulsed X-ray emission is more likely for binary rather than isolated MSPs with the emission arising from the interaction of the relativistic pulsar wind with a binary companion. Our study suggests that the magnetization parameter in the pulsar wind nebulae of MSPs is significantly larger than that of the Crab nebula by about a factor of 10. The emission from MSPs moving at high velocities may appear spatially extended with a tail-like morphology, which may contribute to the faint filamentary X-ray source subpopulation in the Galaxy.

*Subject headings:* binary: close – stars: neutron – X-rays: stars – pulsars: general – radiation mechanisms: thermal – radiation mechanisms: non-thermal

## 1. INTRODUCTION

Millisecond pulsars have been a subject of active interest ever since the discovery of PSR 1937+21 by Backer et al. (1982). It is generally accepted that the neutron stars in these systems have been spun up by accretion torques in binary systems (e.g., Alpar et al. 1984; Phinney & Kulkarni 1994). This class of rotation powered pulsars can remain active for as long as a Hubble timescale, offering the opportunity for investigating the emission processes of old recycled neutron stars. Of interest in recent years have been studies of the X-ray properties of these objects. Specifically, pioneering studies carried out by Becker & Trümper (1999) using ROSAT led to the detection of 9 millisecond pulsars in the energy band from 0.1 - 2.4 keV. Since little X-ray emission is expected from the cooling of the neutron star, due to the millisecond pulsars' long age (e.g., Tsuruta 1998), investigators have primarily focused on emission processes taking place in the magnetosphere (e.g., Cheng & Ruderman 1980; Arons 1981; Zhang & Harding 2000; Harding & Muslimov 2001, 2002; Zhang & Cheng 2003).

However, it has long been recognized that the nebulae surrounding young pulsars are important for understanding the nature and spatial extent of the non-thermal X-ray emission of these compact objects after X-ray detections of the Crab nebula (Peterson & Jacobson 1970 and references therein). In particular, the recent X-ray images of young pulsars obtained with the *Chandra* Observatory have revealed spatially resolved structures, which provide important diagnostic information about the geometry of the inner regions of the Crab supernova remnant (Weisskopf et al. 2000) and Vela nebula (Helfand, Gotthelf, & Halpern 2001). Such extended structures are not limited to young pulsars as they have also been observed from the three million year old pulsar PSR 1929+10 (Becker et al. 2005) and from the old binary millisecond pulsar PSR 1957+20 (Stappers et al. 2003). The information gleaned from these observational studies is vital for facilitating an understanding of the mechanism involved in the production of the X-ray emission. For the majority of pulsars, where the nebulae are unresolved, the wind nebulae would contribute to the non-thermal non-pulsed X-ray emission component (see Kennel & Coroniti 1984; Chevalier 2000). Recently, Cheng, Taam, & Wang (2004) have found that the X-ray properties of the non-thermal non-pulsed emission component of all known rotation powered X-ray pulsars could be interpreted within such a framework whether or not a wind nebula has been identified with the pulsar.

In this paper, we build on the seminal study of the X-ray emission properties of millisecond pulsars elucidated in Becker & Trümper (1999) to examine the properties of the non-thermal non-pulsed component from recycled neutron stars. The origin of the X-ray emission from these objects may be on the neutron star surface, in the magnetosphere,

and in the wind nebula. Since different radiation processes are involved in these spatially distinct regions, it is likely that their contribution to the total luminosity and energy spectra differ. Cheng et al. (2004) argue that the main contribution to the non-thermal non-pulsed component in pulsars is due to the emission from the wind nebula. In this paper, we assume this to be the case as well, although one cannot exclude magnetospheric contributions at luminosity levels lower than  $\sim 3 \times 10^{-4}$  of the spin down power.

Our interest in the X-ray emission of millisecond pulsars has been further stimulated by the recent detection of faint X-ray point sources with luminosities in the range from  $\sim 10^{31} - 10^{35}$  ergs s $^{-1}$  in deep observational surveys of the Galactic center by Wang, Gotthelf, & Lang (2002) and Munro et al. (2003). The spectra of the Galactic center sources in the innermost 20 pc have been fitted to a power law of photon index,  $\Gamma$ , ranging from about -1 to 3 (Munro et al. 2003). Munro et al. (2004) suggest that magnetic cataclysmic variables can substantially contribute to the faint population characterized by hard spectra. On the other hand, these binary systems do not significantly contribute to the fainter X-ray population characterized by softer spectra. Belczynski & Taam (2004) suggest that among neutron star models, the neutron stars in the quiescent state of soft X-ray transients in Roche lobe overflow systems can contribute to the faint ( $10^{31} - 10^{33}$  ergs s $^{-1}$ ), soft sources detected in the Munro et al. (2003) survey. The millisecond pulsars, which are likely descendants of such systems, may contribute more significantly to the general population of such sources in the Galaxy because of their long lifetimes. Estimates of the number of millisecond pulsars in the Galaxy exceeds  $3 \times 10^4$  (Lyne et al. 1998).

Here, we explore millisecond pulsars as a possible class of compact objects contributing to the faint X-ray source population in the Galaxy. In the next section, the X-ray data on millisecond pulsars is collected, illustrating the observational correlations of their X-ray properties. The theoretical basis for these correlations are described in §3 within the framework of a simple model, based on the work by Chevalier (2000) for the wind nebulae surrounding young pulsars. In addition, the emission from an intrabinary shock for the case in which the relativistic pulsar wind interacts with a companion star is also discussed. In §4, the model is applied to the millisecond pulsar B 1957+20 and is used to estimate the pulsar wind contribution to the non-pulsed X-ray luminosity in the millisecond pulsars B1937+21 and J 0218+4232. We also discuss the possible relevance of the emission from the wind nebulae and surrounding environment of millisecond pulsars in the soft X-ray transient SAX J1808.4-3658, the Galactic center, and in the globular clusters 47 Tuc and M28. Finally, we summarize and discuss the implications of the results of our study in the last section.

## 2. OBSERVATIONAL X-RAY PROPERTIES OF MILLISECOND PULSARS

The ROSAT results from the early studies of Becker & Trümper (1993, 1999) suggested that the X-ray radiation from millisecond pulsars is composed of non-thermal and thermal components. The thermal emission was attributed to the heated polar caps and the non-pulsed non-thermal emission to a pulsar wind or a plerion (Becker & Trümper 1993). Observations with the ASCA satellite at energies higher than those accessible by the ROSAT satellite have also revealed the presence of X-ray pulses (Saito et al. 1997b). More recently, Mineo et al. (2000) and Becker & Aschenbach (2002) detected both the pulsed and non-pulsed non-thermal emission components of additional millisecond pulsars based on *BeppoSAX*, *Chandra* and *XMM-Newton* observations. Direct evidence of the spatial X-ray distribution was provided by Stappers et al. (2003) in their important discovery of the nebula surrounding PSR B1957+20.

In Table 1, the luminosities and spectral properties of 8 millisecond pulsars in the Galactic field are collected from recent observations based on X-ray data obtained from the *ASCA*, *RXTE*, *BeppoSAX*, *Chandra* and *XMM-Newton* satellites. For 2 of these pulsars, the pulsed and/or non-pulsed emission components were separately analyzed. As in our previous study (Cheng, Taam, & Wang 2004), we assume that the pulsed component arises from the pulsar magnetosphere and that the non-thermal non-pulsed component is due to a pulsar wind nebula.

The relation between the total X-ray luminosity and the spin down power of the 8 millisecond pulsars, as obtained from the literature, is illustrated in Fig. 1. A correlation between the total X-ray luminosity in the energy range of 2-10 keV,  $L_x^{tot}$ , and the spin down power,  $\dot{E}$ , is seen to be present, and it is described by the best fit function  $L_x \propto \dot{E}^{1.39 \pm 0.08}$  ergs  $s^{-1}$ , where we have approximated the errors in  $\log(L_x)$  to be  $\pm 0.2$ . This relation was first discovered by Seward & Wang (1988) with Einstein data and others have also found similar correlations of normal and millisecond pulsars taken together (e.g. Ögelman 1995; Saito 1998; Cheng, Taam & Wang 2004). Becker & Trümper (1997), using ROSAT data in the energy range of 0.1-2.4 keV, found a slightly different relation ( $L_x \propto \dot{E}^{1.03 \pm 0.08}$ ). In the energy range analyzed by Becker & Trümper (1997), the thermal component, which is expected to be emitted from the neutron star surface, can play a significant role. On the other hand, the thermal component should not significantly contribute in our selected energy range (2-10 keV). This suggests that there could be another component contributing to the harder X-rays. Cheng, Taam & Wang (2004) have used the ASCA data of both normal and millisecond pulsars to analyze the relations between the  $\dot{E}$  and the total X-ray luminosity, pulsed X-ray luminosity ( $L_x^{pul}$ ), and non-pulsed X-ray luminosity ( $L_x^{npul}$ ). The relations between  $L_x^{tot} - \dot{E}$  and  $L_x^{npul} - \dot{E}$  are found to be very similar, whereas the relation

between  $L_x^{pul} - \dot{E}$  is similar to the relation obtained by Becker & Trümper (1997). It was shown that the latter relation results from magnetospheric radiation, but that the non-pulsed radiation likely originates from the pulsar wind nebula (PWN). Since ASCA has a large collection area, which should cover the pulsar wind shock radiation region, a significant fraction of the total luminosity could be contributed by the PWN. Although we do not have a sufficient number of millisecond pulsars to carry out the non-pulsed X-ray luminosity analysis, we hypothesize that the pulsar wind nebula is a significant contributor to the total luminosity in 2-10 keV range.

The measured photon power law indices,  $\Gamma$ , of the total X-ray emission are found in the range from  $\sim 0.6 - 3$  (see Table 1). For the millisecond pulsars in which the photon index of the pulsed and non-pulsed components were determined, it appears that the spectral indices of their non-pulsed emission range from 3.3 for B1937+21 to 1.17 for J0218+4232.

### 3. THEORETICAL PROPERTIES OF X-RAY EMISSION FROM MILLISECOND PULSARS

The X-ray emission from a pulsar can arise from various processes on the neutron star surface or in its vicinity. For example, thermal processes can occur on its surface and polar cap regions, synchrotron emission processes within its magnetosphere and synchrotron processes in the shocked region resulting from the interaction of a relativistic wind with a binary companion to the pulsar or the surrounding interstellar medium. It should be pointed out that curvature radiation and the inverse Compton processes can also contribute to the radiation from the pulsar magnetosphere and pulsar wind nebula. However, these two processes can only generate  $\gamma$ -rays. For example, in the case of the intrabinary shock, it has been shown that although the inverse Compton scattering can be the dominant cooling process, it will produce a Maxwellian spectrum with a peak energy at several tens of GeV (Tavani, Arons & Kaspi 1994; Tavani & Arons 1997). In this paper we focus on the X-ray emission, and, therefore we will ignore these two processes. In the following, we discuss the various emission processes in turn.

#### 3.1. Emission inside the light cylinder

As thermal X-ray emission from the entire neutron star surface is not expected to be appreciable due to the age of the pulsar, the thermal X-ray emission from the neutron star surface is likely to be limited to a polar cap region. For simplicity, we assume that the

thermal X-ray luminosity is given as  $L_{X,\text{th}} \simeq \dot{N}V_{\text{gap}}$ . Here,  $\dot{N} \sim 1.35 \times 10^{30} B_{12} P^{-2} \text{e s}^{-1}$  (Goldreich & Julian 1969), and  $V_{\text{gap}}$  is the potential of the polar gap. Jones (1980) showed that the photoejection of the most tightly bound electrons of ions can limit the potential of the polar gap to  $V_{\text{gap}} = \gamma(A/Z)10^9 \text{ V}$  where  $A/Z \sim 2$  and  $\gamma$  is the Lorentz factor of ions. Cheng & Taam (2003) argue that if higher order magnetic fields are present on the surface of neutron star  $\gamma \sim 20$ . For the typical parameters of millisecond pulsars in the Galaxy (e.g.  $P = 3 \text{ ms}$ ,  $B = 2 \times 10^8 \text{ G}$ ),  $L_{X,\text{th}} \sim 10^{30} \text{erg s}^{-1}$ .

In contrast to the thermal processes taking place on the neutron star surface, non-thermal X-rays can be produced in its immediate vicinity as a result of synchrotron emission of electron-positron pairs produced by an electromagnetic cascade near the neutron star surface (see Cheng, Gil & Zhang 1998; Cheng & Zhang 1999; Zhang & Cheng 2003). The model predicts a luminosity  $\sim 2.5 \times 10^{-9} \dot{E}^{1.15}$  (Cheng & Zhang 1999). The conversion efficiency of spin down power to photon luminosity in the energy range from 0.1 keV to 1 MeV is  $\sim 3 \times 10^{-4}$ .

### 3.2. Pulsar wind nebulae in the interstellar medium

The non-thermal X-ray radiation can also be produced as a result of synchrotron emission processes in a region affected by the interaction of the pulsar’s relativistic wind with the interstellar medium. The resulting interaction can take the form of a termination shock. A detailed description of the interaction between a pulsar and its nebula, as applied to the Crab Nebula, was first outlined in a seminal paper by Rees and Gunn (1974). Theoretical studies on the X-ray emission from PWN have remained as an important topic due to the increased quality of observed data. Blondin, Chevalier & Frierson (2001) have used one- and two-dimensional two fluid models to simulate the PWN in evolved young supernova remnants. This model can explain some chaotic and asymmetric appearances of young PWN such as the Vela Nebula. Bucciantini (2002) has used a 2D hydrodynamic model to estimate the opacity of the bow-shock to penetration of ISM neutral hydrogen, which can significantly affect the size, shape, velocity and brightness distribution of the nebula. A magnetohydrodynamical model was developed by van der Swaluw (2003) to simulate the expansion of PWN, showing that the PWN is elongated as a result of the dynamical effect of toroidal magnetic fields. Finally, Komissarov & Lyubarksi (2003) have used a 2D relativistic magnetohydrodynamical model to simulate the peculiar jet-torus structure of the Crab nebula. For a recent discussion of the emission characteristics of the shocked region, see Cheng et al. (2004). In this subsection, we will use a simple spherically symmetric (1D) model similar to that suggested by Chevalier (2000) to estimate

the non-thermal radiation from the PWN of MSP. In general, 2D or 3D models are necessary to provide a detailed theoretical explanation of the emission morphology from young pulsars (Gaensler 2004). However, the proper motion of MSPs are typically much slower than canonical high magnetic field pulsars. The PWN of MSP may be older and expanding more slowly (subsonically). Furthermore, we can estimate the distance from the neutron star where the charged particles in the pulsar wind can break away from the pulsar magnetic field by requiring that the Larmor radius of the particle becomes larger than the curvature radius of the magnetic field. This requirement leads to a break away radius at  $r_{break} \sim \frac{qR^3 B_s \Omega}{cE_p}$ , where  $B_s$  is the surface magnetic field,  $R$  is the stellar radius and  $E_p \sim \gamma_w m_p c^2$  is the mean energy of the charged particle in the wind. Although the toroidal magnetic fields of young pulsars in PWN could indeed have a dynamical influence on its structure, making the nebula elongated (e.g. van der Swaluw 2003), the magnetic field strengths of MSPs are much weaker and may not be as effective. From the above estimate, we can see that this is true if the mean Lorentz factor in the pulsar is a constant. Cheng, Taam and Wang (2004) have argued that the relation between the X-ray luminosity and the pulsar spin-down power ( $\dot{E}$ ) can be obtained if  $E_p \propto \dot{E}^{1/2}$ . Since  $B_s \Omega^2 \propto \dot{E}^{1/2}$ , then  $r_{break} \propto 1/\Omega$ , providing additional evidence that the nebula of MSP is not as elongated as in the young pulsars. Consequently, the bow shock created by MSP may be well approximated by a 1D model.

For isolated millisecond pulsars, the radius of the bow shock (which is expected to be comparable to the size of the X-ray emitting region) produced by the interaction of the pulsar wind with the interstellar medium is obtained from a pressure balance condition, leading to

$$R_s = (\dot{E}/2\pi\rho v_p^2 c)^{1/2} \sim 1.8 \times 10^{16} \dot{E}_{34}^{1/2} n^{-1/2} v_{p,100}^{-1} \text{cm}, \quad (1)$$

where  $v_{p,100}$  is the pulsar velocity in units of 100 km s<sup>-1</sup>,  $\dot{E}_{34}$  is the spin down power of the pulsar in units of 10<sup>34</sup> ergs s<sup>-1</sup>, and  $n$  is the number density of the interstellar medium in units of 1 cm<sup>-3</sup>. We point out that the size of PWN is energy dependent since the cooling time in X-rays is shorter than in the radio regime. Since it is very likely that the synchrotron cooling time in X-ray energy range is shorter than the flow time in the shock region, the X-ray PWN can be approximated by Equation 1. On the other hand, the TeV PWN should be larger than that of X-ray PWN because when the relativistic electrons leave the shock region (while radiating at lower frequencies), they contribute to the TeV photon production via the inverse Compton scattering process.

In the shock wave, the energy can be stored in the proton (ion), electron, and magnetic field components. The fractional energy densities  $\epsilon_p$ ,  $\epsilon_e$ , and  $\epsilon_B$  correspond to that of the protons, electrons, and magnetic field respectively. We note that the protons do not contribute to the X-ray emission through the synchrotron process. The energy densities

in the shock are not theoretically determined with any certainty, however, Kennel & Coroniti (1984) have argued that only for ratios of magnetic to kinetic energy, defined as  $\sigma_B \sim \epsilon_B/(\epsilon_p + \epsilon_e)$ , less than about 0.1 can a significant fraction of total energy flux upstream be converted into thermal energy downstream and, thereafter, into synchrotron luminosity. In fitting to the observational data of the Crab nebula, Kennel & Coroniti (1984) found that  $\sigma_B$  should lie in the range between 0.001 and 0.01. deJager & Harding (1992) have found that  $\sigma_B = 0.003$  gives the best fit for the EGRET and TeV data from the Crab nebula. Recently, Sefako & deJager (2003) have found that the broadband spectrum of a PWN crucially depends on the magnetization parameter, spin-down power, distance, particle multiplicity and shock radius. In order to fit the broadband spectrum of the Vela pulsar and PSR B1706-44, the best fit value of  $\sigma_B = 0.1$  was found for these pulsars, both of which have very similar ages ( $\sim 5 \times 10^3$  years). This value is substantially different from that of the Crab nebula. Since the Crab nebula has been observed and theoretically studied more than any other pulsar wind nebula, we adopt  $\sigma_B=0.003$  as the standard reference value, but we also consider other possible value of  $\sigma_B$ . In addition, we also assume comparable particle kinetic energy fractions (e.g.  $\epsilon_p$  and  $\epsilon_e \sim 0.5$ ) throughout this study. Thus, the magnetic field in the emitting region can be estimated as

$$B = (6\epsilon_B \dot{E}/R_s^2 c)^{1/2} \sim 5 \times 10^{-6} (\epsilon_B/0.003)^{1/2} n^{1/2} v_{p,100} G. \quad (2)$$

Following the analysis of Chevalier (2000, see also Cheng et al. 2004), the X-ray properties of the pulsar wind can be theoretically calculated. In particular, we take the postshock electron energy distribution for a strong relativistic shock as  $N(\gamma) \propto \gamma^{-p}$  for  $\gamma > \gamma_m$ , where  $\gamma_m = \frac{p-2}{p-1} \epsilon_e \gamma_w$ , and  $\gamma_w$  is the Lorentz factor of the relativistic pulsar wind, which is assumed to be  $10^6$  throughout this study.

The determination of the X-ray luminosity is dependent on the cooling frequency,  $\nu_c$ , given as  $\nu_c = \frac{e}{2\pi m_e c B^3} (\frac{6\pi m_e c}{\sigma_T t})^2$ , where  $t$  is a characteristic timescale of the nebula estimated as the flow timescale in a characteristic radiation region, i.e,  $t \sim R_s/v_p$ . For  $\nu_X > \nu_c$  (denoted as fast cooling), the observed luminosity of radiating particles per unit frequency is given as (Chevalier 2000)

$$L_\nu = \frac{1}{2} \left(\frac{p-2}{p-1}\right)^{p-1} \left(\frac{6e^2}{4\pi^2 m_e c^3}\right)^{(p-2)/4} \epsilon_e^{p-1} \epsilon_B^{(p-2)/4} \gamma_w^{p-2} R_s^{-(p-2)/2} \dot{E}^{(p+2)/4} \nu^{-p/2}. \quad (3)$$

Here, we estimate the total X-ray luminosity as  $\nu L_\nu$  for simplicity. Taking typical parameters for millisecond pulsars ( $P = 3$  ms,  $B = 2 \times 10^8$  G,  $\dot{E} \sim 10^{34}$  ergs s<sup>-1</sup>,  $v_p \sim 180$  km s<sup>-1</sup> and  $n \sim 1$ cm<sup>-3</sup>,  $\epsilon_e \sim 0.5$ ,  $\epsilon_B \sim 0.003$ ,  $\gamma_w \sim 10^6$ , and  $p = 2.2$  (we take the possible

optimum value based on theoretical investigations of highly relativistic shock fronts in the limit of high Lorentz factors, see Bednarz & Ostrowski 1998, Lemoine & Pelletier 2003), the X-ray luminosity ( $\nu \sim 10^{18}\text{Hz}$ ) is  $\nu L_\nu \sim 4 \times 10^{30}\text{ergs s}^{-1}$ . In order to explain the observed relation between the X-ray luminosity and the spin-down power, we (Cheng, Taam & Wang 2004) have argued that  $\gamma_w \sim 5 \times 10^3 B_{12}/P^2 \sim 2 \times 10^5 (B/3 \times 10^8 G)/(P/3ms)^2$ . For  $\gamma_w = 2 \times 10^5$  and  $\epsilon_B \sim 0.1$ ,  $\nu L_\nu$  will decrease slightly to  $\sim 3.3 \times 10^{30}\text{ergs s}^{-1}$ . If we decrease  $p$  to slightly larger values than  $\sim 2$ , the luminosity reaches a level of  $\sim 4 \times 10^{31}\text{ergs s}^{-1}$ . In this regime, the efficiency of conversion of spin down power to X-ray luminosity can be as high as  $\sim 4 \times 10^{-3}$ , a value which is much greater than that associated with the pulsed emission from the magnetosphere (cf. §3.1). As is well known, the photon index in the fast cooling regime is given by  $\Gamma = (p + 2)/2$ . Generally,  $p$  can vary from 2 to 3, and the pulsar wind nebulae could produce non-thermal spectra with photon indices in the range from 2 to 2.5. On the other hand, if the cooling frequency is larger than the frequency  $\nu_X$  (denoted as slow cooling), the observed luminosity per frequency  $L'_\nu \sim (\nu/\nu_c)^{1/2} L_\nu \propto \nu^{-(p-1)/2}$ . In this regime, the X-ray luminosity will be lower than that in the fast cooling regime, and the observed photon index is  $\Gamma = (p + 1)/2$  (Chevalier 2000). In this case, the pulsar wind nebulae could produce non-thermal spectra with photon indices ranging between 1.5 and 2, corresponding to conversion efficiencies ranging from about  $2 \times 10^{-6}$  to  $9 \times 10^{-5}$  for the parameters used in the fast cooling case (see above).

In principle, the theoretical model can be tested using the observed X-ray luminosity, the size of the X-ray emission region ( $\sim R_s$ ), and Eq. 3 to solve for the value of  $p$  to determine if it is within the theoretical allowed range, thus providing a consistent estimate of  $\Gamma$  in comparison with the observed spectral index. However, a spectral index has to be assumed to infer the observed X-ray luminosity. In other words,  $\Gamma$  and  $L_x$  are not independent. Furthermore, the errors in  $L_x$  and  $R_s$  do not provide an accurate estimate of  $p$ . Therefore, it is more practical to choose a possible value of  $p$  with the constraint of theories (e.g. Bednarz & Ostrowski 1998, Lemoine & Pelletier 2003) to estimate  $L_x$  and  $\Gamma$  for comparison with those observed. We remark that since shock acceleration is a non-linear process, it would not be surprising that various observations lead to a range of  $p$ . In the following applications, we will treat  $p$  as a parameter but with the constraint that it should only vary between 2 and 3 as suggested by theoretical studies (e.g. Bednarz & Ostrowski 1998, Lemoine & Pelletier 2003).

### 3.3. Emission from the intrabinary shock

Non-thermal radiation can also arise from a shock wave resulting from the interaction between the pulsar wind and the outflowing matter from the companion star (Arons & Tavani 1993, Stella et al. 1994, Tavani & Arons 1997). In this context, the neutron star is at a distance,  $D$ , from the surface of its binary companion given by  $D = R + R_s$ , where  $R_s$  is the shock wave termination radius as measured from the neutron star surface and  $R$  is the distance of the shock from the surface of the companion star. For millisecond pulsars in binary systems with low mass companions, we adopt an orbital separation  $\sim 2 \times 10^{11}$  cm. If we assume that mass is lost isotropically from the companion star, the loss rate is given as  $\dot{M} = 4\pi\rho(R_* + R)^2v_w$ , where  $v_w$  is its outflow velocity and  $\rho$  is the density at distance  $R$  from the stellar surface and  $R_*$  is the radius of the companion. The dynamic outflow pressure given by  $P_w(R) = \rho(R)v_w(R)^2$  can be expressed as

$$P_w(R) = \frac{\dot{M}v_w}{4\pi(R_* + R)^2}. \quad (4)$$

The termination radius of the pulsar wind is given by the pressure balance between the pulsar and companion outflow and can be expressed as

$$\left(\frac{R_s}{R_* + R}\right)^2 = \frac{\dot{E}}{\dot{M}v_w c}. \quad (5)$$

In order to estimate the shock radius,  $\dot{M}$  and  $v_w$  must be determined. Unlike the case of the progenitor of millisecond pulsars, i.e., the low mass X-ray binaries, where  $\dot{M}$  can be estimated from the X-ray accretion luminosity, the mass loss rate from the neutron star companion likely results from the evaporation by a pulsar wind (Ruderman, Shaham & Tavani 1989). If the stellar wind is a consequence of evaporation by the pulsar wind, the balance between the stellar wind pressure and the pulsar wind pressure lies near the position of the companion, implying  $R_s \sim D$ . In taking PSR B1957+20 as an example, we find that  $R_s > 0.6(R_* + D)$  under the assumption that the wind velocity is comparable to the escape speed from the companion and the mass loss rate is  $\lesssim 10^{17}$  g s<sup>-1</sup> (see Stappers et al. 2003).

The cooling frequency  $\nu_c$  is given as  $\nu_c = \frac{e}{2\pi m_e c B^3} \left(\frac{6\pi m_e c}{\sigma_T t_f}\right)^2$ , where  $t_f \sim \sqrt{3}R_s/c$  is the dynamical flow time and the magnetic field strength at the termination radius is estimated by  $B = (6\epsilon_B \dot{E}/R_s^2 c)^{1/2}$ . Taking  $\dot{E} \sim 10^{35}$ ,  $\epsilon_B \sim 0.003$ , and  $R_s \sim 10^{11}$  cm, we obtain  $\nu_c \sim 3 \times 10^{21}$  Hz. Since the cooling frequency is much larger than the frequency  $\nu_x \sim 10^{18}$  Hz, the observed luminosity per frequency  $L_\nu \propto \nu^{-(p-1)/2}$ . Based on the work by Chevalier (2000), the total X-ray luminosity radiated in the intrabinary shock wave for a solid angle of  $\Omega$  toward the pulsar is estimated as

$$\nu L_\nu = \frac{\Omega}{4\pi} \frac{\sigma_T 6^{(p-3)/4} (p-2)^{p-1}}{2\pi m_e c^{(p+5)/4} (p-1)^{p-2}} \left( \frac{e}{2\pi m_e c} \right)^{(p-3)/2} \epsilon_e^{p-1} \epsilon_B^{(p+1)/4} R_s^{-(p+1)/2} \gamma_w^{p-2} t_f \dot{E}^{(p+5)/4} \nu^{-(p-3)/2}, \quad (6)$$

in the X-ray energy band (2-10 keV). It is interesting to note that if we approximate  $t_f \sim \sqrt{3}R_s/c$  and  $R_s = D$ , the above equation can be rewritten as

$$\nu L_\nu = 5 \times 10^{30} \alpha(p) f_{0.1} D_{11}^{-(p-1)/2} \dot{E}_{35}^{(p+5)/4} \text{ ergs s}^{-1}, \quad (7)$$

for  $\nu = 10^{18} \text{ Hz}$ ,  $\gamma_w = 10^6$ ,  $\epsilon_e = 0.5$ ,  $\epsilon_B = 0.003$  and  $\alpha(p)$  is a function of  $p$ , which only varies from 1 to 2.6 as  $p$  increases from 2.2 to 2.6. For simplicity, we may assume it is a constant of order of unity. Here,  $f = \Omega/4\pi$ ,  $D_{11} = D/10^{11} \text{ cm}$  and  $\dot{E}_{35} = \dot{E}/10^{35} \text{ ergs s}^{-1}$ . We note that Tavani & Arons (1997) have estimated that  $\epsilon_B \sim 0.02$  in the intrabinary shock region in order to explain the X-ray emission from PSR 1259-63. For this value, the coefficient in Equation 7 will change to  $3 \times 10^{31}$ .

Thus, the emission from the intrabinary shock is expected to be in the slow cooling regime characterized by a photon index,  $\Gamma = (p+1)/2$ , while the emission from the pulsar interaction with the interstellar medium can be either in the slow or fast cooling regime.

## 4. APPLICATIONS

### 4.1. Pulsar Wind Nebula Source

#### 4.1.1. PSR B1957+20

In a recent study by Stappers et al. (2003) an X-ray nebula in the vicinity of the millisecond pulsar B1957+20 was detected. A bright X-ray source in the field was found to be coincident with the pulsar position, and a tail of X-ray emission was seen extending from the pulsar to the northeast by at least  $16''$  (corresponding to  $\sim 4 \times 10^{17} \text{ cm}$  at the distance of 1.5 kpc) at a position angle opposite to the pulsar's direction of motion. Taken together with the existence of a previously identified  $\text{H}\alpha$  bow shock structure (Kulkarni & Hester 1988) enveloping this tail, PSR B1957+20 is a prime example of an X-ray bow shock nebula in a pulsar binary system. PSR B1957+20 is the second fastest spinning pulsar known, with a rotation period of 1.6 ms and a rotational spin-down luminosity of  $\simeq 10^{35} \text{ erg s}^{-1}$  (Fruchter et al. 1988, Toscano et al. 1999). It is a member of a binary system ( $P = 9.16$  hour) with a low mass companion star separated by a distance of  $1.5 \times 10^{11} \text{ cm}$ . Since PSR B1957+20 has a non-thermal X-ray spectrum ( $\Gamma = 1.9 \pm 0.5$ ), it is likely that the

pulsar wind interaction with the companion and the interstellar medium, and the pulsar’s magnetosphere contribute to the unresolved emission. Stappers et al. (2003) argue that the unresolved X-ray emission originates from the interaction between the pulsar wind and the induced stellar wind of its companion, and that the resolved emission in the tail is a result of the interaction between the pulsar wind and the interstellar medium.

The tail is characterized by a length  $l \gtrsim 4 \times 10^{17}$  cm and an X-ray luminosity of  $\sim 2.4 \times 10^{30}$  ergs  $s^{-1}$ . We interpret its length in terms of the distance traversed by the pulsar within the electron synchrotron cooling timescale, i.e.  $l \sim v_p t_c$  where  $v_p$  is the proper motion velocity of the pulsar. The magnetic field strength in the region surrounding the pulsar can be roughly estimated by assuming a compression of the interstellar magnetic field ( $\sim 2 - 6 \mu\text{G}$ ; see Beck et al. 2003). For a field compression in the termination shock of a factor of 3 (Kennel & Coroniti 1984), the inferred field is  $\sim 6 - 18 \mu\text{G}$ . The synchrotron cooling time in the X-ray band is  $\tau_c = 6\pi m_e c / \gamma \sigma_T B^2 \sim 10^8 B_{mG}^{-3/2} (h\nu_X / \text{keV})^{-1/2}$  s, yielding  $\tau_c$  in the range of 1400-7100 yrs. Since the length of the tail is energy dependent, we have chosen a representative X-ray energy at KeV in order to compare with the observations. The pulsar moves through the interstellar medium at  $220 \text{ km s}^{-1}$  (Arzoumanian et al. 1994), and the inferred tail length is  $\sim 9 \times 10^{17} - 4.6 \times 10^{18}$  cm, suggesting that the higher inferred magnetic field is more appropriate. Alternatively, equating the observed tail length to the product of the synchrotron cooling timescale and the pulsar velocity leads to  $B \sim 30 \mu\text{G}$  or a factor of 1.67 higher than the previously estimated value.

For a number density  $\sim 1 \text{ cm}^{-3}$ , consistent with the hydrogen column density inferred from the X-ray observations (Stappers et al. 2003), the termination shock radius of PSR B1957+20 is estimated to be  $\sim 2.5 \times 10^{16}$  cm, which corresponds to an angular extent of  $\sim 1''$ . Given  $B_{mG} = 0.03$  (see above), we estimate that the cooling frequency is lower than the X-ray frequency. Based on the results in §3.2 the spectral index of the nebula component is then  $\Gamma = (p + 2)/2$ . Taking  $p = 2.3$ ,  $\epsilon_B \sim 0.003$ ,  $\epsilon_e \sim 0.5$  and  $\gamma_w = 10^6$ , and  $R_s \sim 2.5 \times 10^{16}$  cm, the predicted nebula luminosity (0.5-7 keV) is  $\sim 5 \times 10^{30} \text{ erg s}^{-1}$ . If we choose  $\epsilon_B \sim 0.1$  and  $\gamma_w = 5 \times 10^5$ , then the luminosity increases to  $7 \times 10^{30} \text{ erg s}^{-1}$ . This value is higher than the observed luminosity in the tail by a factor of about 3, suggesting that some of this emission may contribute to the unresolved emission (see below).

The X-ray luminosity of the unresolved source in an aperture radius  $1.5''$  is  $\sim 1.6 \times 10^{31} \text{ erg s}^{-1}$ , and Stappers et al. (2003) suggest that it is produced in an intrabinary shock between the pulsar wind and that of the companion star. According to the estimates given in §3.3, the X-ray luminosity (0.5-7 keV) from the intrabinary shock, which contributes to the unresolved component, is about  $\sim 5 \times 10^{30} \text{ erg s}^{-1}$  assuming  $p = 2.3$ ,  $\epsilon_B \sim 0.003$ ,  $\epsilon_e \sim 0.5$ ,  $\gamma_w = 10^6$ , and  $\Omega = 1$ . Again choosing  $\epsilon_B \sim 0.1$ ,  $\gamma_w = 5 \times 10^5$ ,

the X-ray luminosity from the intrabinary shock increases significantly to  $\sim 6 \times 10^{31} \text{erg s}^{-1}$ . In order to fit the observation,  $\epsilon_B \sim 0.02$ . This value is consistent with the value obtained by Tavani & Arons (1997) for PSR1259-63, where the X-rays and  $\gamma$ -rays also result from intrabinary shock.

From the above estimates, it is evident that the pulsar wind nebula could contribute to the flux of both the unresolved X-ray source as well as to the X-ray tail since the termination radius ( $R_s \sim 2.5 \times 10^{16} \text{cm}$ ) subtends an angle comparable to the *Chandra* angular resolution. In this case, the pulsar wind interaction with the interstellar medium would contribute significantly to the flux of the unresolved X-ray source. With the contribution from the intrabinary shock interaction, the total predicted nebula X-ray luminosity would amount to  $\sim 1.4 \times 10^{31} \text{erg s}^{-1}$ , which is consistent with the observed value.

Becker & Trümper (1997,1999) have suggested that the X-ray luminosity in the range of 0.2-2.4 keV of rotation powered pulsars should satisfy  $L_x \sim 10^{-3} \dot{E}$ . This relation predicts that the X-ray luminosity in the 2-10 keV energy range to be a factor of  $5_{+6}^{-3}$  larger than observed assuming a photon index  $\Gamma = 1.9 \pm 0.5$ . Cheng & Taam (2003) have argued that if there are higher order magnetic fields present on the surface of millisecond pulsars, the non-thermal X-rays as well as gamma-rays will be suppressed. In this case, the thermal X-ray luminosity from the polar cap heating will be reduced to  $\sim 3 \times 10^{30} \text{ergs s}^{-1}$  as suggested in §3.1.

#### 4.1.2. PSR B1937+21 and J0218+4232

Of the millisecond pulsars listed in Table 1, only PSR B1937+21 and J0218+4232 have measured power law photon indices for both the pulsed and non-pulsed emission components, partly because they have a larger spin down power and higher X-ray luminosity than the other millisecond pulsars. Although pulsar wind nebulae have not been imaged in these two millisecond pulsars, it is possible that the non-thermal, non-pulsed components are produced within such regions. In this subsection, we explore the consequences of pulsar wind nebulae surrounding these millisecond pulsars as the candidate sites for this X-ray emission component.

The velocities of PSR B1937+21 and J0218+4232 are still unknown or quite uncertain. Since the average birth velocities of observed millisecond pulsars are  $\sim 130 \text{km s}^{-1}$  (Lyne et al. 1998), we adopt this value as their typical velocity. Assuming that the surrounding medium has a density of  $\sim 1 \text{cm}^{-3}$  and using the spin down power listed in Table 1, the

termination radius of the bow shocks in the hypothesized nebulae are  $\sim 2 \times 10^{17}$  and  $\sim 10^{17}$  cm for B1937+21 and J0218+4232 respectively. Taking a conservative value of  $\epsilon_B \sim 0.003$ , the magnetic field is estimated to be  $\sim 10^{-5}$  G, and the cooling frequencies of the nebulae are given as  $\sim 3.6 \times 10^{19}$  Hz for B1937+21 and  $1.4 \times 10^{20}$  Hz for J0218+4232. Since  $\nu_c > \nu_X$ , we find the nebulae would be in the slow cooling regime. As a result, the simple one-zone model outlined in §3 indicates that their photon spectral indices,  $\Gamma = (p + 1)/2$ , are generally smaller than 2. The observed non-pulsed photon index of PSR B1937+21 is  $3.3 \pm 0.5$ , which should be more consistent with the fast cooling region. In this case if we take  $\epsilon_B \sim 0.1$ , the cooling frequencies of the nebulae are given as  $\sim 1.8 \times 10^{17}$  Hz for B1937+21 and  $7.2 \times 10^{17}$  Hz for J0218+4232 respectively. This means  $\nu_c < \nu_X$  and these systems are in fast cooling regime. Furthermore, its non-pulsed component is likely contaminated by the thermal component and the actual photon index for non-thermal emission may be closer to 2, which implies  $p \sim 2.3$ . In this case, the predicted X-ray luminosity and the observed data would be consistent. On the other hand, the observed non-pulsed photon index of PSR B0218+4232 is  $1.17 \pm 0.37$ , which indeed is in slow cooling region. If we adopt the typical value of  $p = 2.3$ , the predicted X-ray luminosity is  $\sim 7 \times 10^{31}$  ergs  $s^{-1}$ , which is higher than the observed value by a factor of 2.5. Since estimates of the distance to J0218+4232 could be as large as 5.7 kpc (Cordes & Lazio 2002), the discrepancy may not be as large as implied. Given the simple model that we have adopted and the sensitivity of the luminosity to the power law index of the electron energy distribution, it is encouraging that the luminosities from the one zone model are of the same order as observed.

#### 4.1.3. PSR J2124-3358

PSR J2124-3358 was discovered during the Parkes 346 MHz survey by Bailes et al. (1997), and X-ray emission was subsequently detected in ROSAT HRI data by Becker & Trümper (1998, 1999). This pulsar has a period of 4.93ms and is characterized by a surface magnetic field of  $2.6 \times 10^8$ G, which gives a spin-down power  $4.4 \times 10^{33}$  erg  $s^{-1}$ . The estimated distance, based on the dispersion measure, is 250pc, and the proper velocity is  $58 \text{ km s}^{-1}$  (Manchester et al. 2005). Very recently the X-ray luminosity associated with a PWN was reported by Hui & Becker (2005). The observed X-ray luminosity associated with the nebula is estimated to be  $\sim 10^{29}$  ergs  $s^{-1}$ , and the spectrum was fitted with a photon power index of  $2.2 \pm 0.3$ . The X-ray emission extends from the pulsar to the northwest by  $\sim 1$  arcmin, which corresponds to a linear scale of  $\sim 2 \times 10^{17}$  cm. The time scale for the passage of the pulsar over this length is about 1,100 years. Assuming that such an X-ray tail results from the finite synchrotron life time effect, we can estimate the magnetic field in the X-ray emission region, which gives  $B \sim 20 \mu\text{G}$ . Although this value is larger than the

typical magnetic field in the interstellar medium of  $2\text{-}6\mu\text{G}$  (Beck et al. 2003), it is consistent with the fact that the magnetic field in the termination shock can be enhanced by a typical factor of 3 (Kennel & Coroniti 1984). With this magnetic field we estimate a cooling frequency of  $\sim 2 \times 10^{17}\text{Hz}$ , which suggests that the X-ray emission is in fast cooling regime. The observed photon index suggests that  $p \sim 2.3$ . For  $\epsilon_B \sim 0.003$ ,  $\epsilon_e \sim 0.5$  and  $\gamma_w = 10^6$ , the estimated X-ray luminosity is  $2 \times 10^{29}\text{ ergs s}^{-1}$ , while for  $\epsilon_B \sim 0.1$  and  $\gamma_w = 2 \times 10^5$ , it is  $1.6 \times 10^{29}\text{ ergs s}^{-1}$  indicating that the X-ray luminosity is not sensitive to these chosen parameters. We note that these luminosity estimates are consistent with the observed data (Hui & Becker 2005).

## 4.2. POTENTIAL PULSAR WIND NEBULA SOURCES

### 4.2.1. SAX J1808.4-3658

SAX J1808.4-3658 was the first low-mass X-ray binary system discovered in which the accreting pulsar exhibited coherent pulsations at a spin period ( $\sim 2.5\text{ ms}$ ) comparable to that observed in millisecond pulsars (Wijnands & van der Klis 1998). The source is a soft X-ray transient (SXRT) which reaches a maximum X-ray luminosity of  $\sim 2 \times 10^{36}\text{ ergs s}^{-1}$  (for a distance of 2.5 kpc; in 't Zand et al. 2001). *XMM-Newton* observations of SAX J1808.4-3658 were obtained during its quiescent state, revealing an unabsorbed luminosity (0.5-10 keV) of  $5 \times 10^{31}\text{ erg s}^{-1}$ , and a spectrum which is characterized by a hard power law with photon index  $\Gamma \sim 1.5 \pm 0.5$  and a minor contribution ( $\leq 10\%$ ) from a soft blackbody component (Campana & Stella 2003). SAX 1808.4-3658 is distinguished from other SXRTs in quiescence by the fact that the power law component is dominant (Campana & Stella 2003).

Jonker et al. (2004) point out that the relative contribution of the hard component to the total flux from neutron stars in SXT systems in the quiescent state may be correlated with the quiescent state X-ray luminosity level with a greater contribution at lower quiescent X-ray luminosities. However, the power law component for Aql X-1 is dominant, even though the quiescent luminosity is  $\sim 2 - 4 \times 10^{33}\text{ ergs s}^{-1}$ , suggesting that the origin of the power law component may differ between sources at high and low quiescent X-ray luminosities (Jonker et al. 2004). Although the origin of this emission is unknown, it is possible that the power law component for more luminous quiescent sources arises, for example, from accretion onto the neutron star whereas the power law component for low luminosity quiescent sources may arise from the activation of the pulsar mechanism when the accretion rate is significantly reduced (see Campana et al. 1998). If the pulsar mechanism is operative and a relativistic wind is established, contributions

to the luminosity and spectrum could involve the interaction between the pulsar wind with the interstellar medium and with a stellar wind of the companion star, the latter analogous to that discussed for B 1957+20 and for PSR J0024-7204W in 47 Tuc (see below; Bogdanov, Grindlay, & van den Berg 2005). Indirect evidence for the possible existence of a relativistic wind in SAX J1808.4-3658 is provided by the requirement of an additional energy source to explain the optical emission during the quiescent state (see Campana et al. 2004). The inferred magnetic field strength of SAX J1808.4-3658 is in the range of  $\sim 10^{8-9}$  G range (see Psaltis & Chakrabarty 1999), leading to a pulsar spin down power of  $\dot{E} \sim 1.8 \times 10^{31} B_{12}^2 P^{-4} \text{ergs s}^{-1} \sim 6 \times 10^{34-36} \text{erg s}^{-1}$ . If the efficiency of conversion of spin-down power to X-ray luminosity is  $\sim 10^{-5} - 10^{-4}$ , in the range found for pulsars with small values of  $\Gamma$  (see Cheng et al. 2004), the luminosity level due to the interaction of the pulsar wind with the interstellar medium could be consistent with that observed. Such an interpretation would suggest that the pulsar in SAX 1808.4-3658 is in the slow cooling regime. A measurement of the space velocity of the system would provide an estimate of the cooling frequency, yielding an independent check on the consistency of this interpretation.

#### 4.2.2. Galactic Center

Deep *Chandra* X-ray surveys have led to the discovery of a number of point-like and tail-like sources in the region of the Galactic center (Wang et al. 2002; Munro et al. 2003). Since the resolution limit of the *Chandra* observations is  $\sim 1''$ , the tail-like sources are characterized by length scales exceeding  $10^{17}$  cm. Such tails may be similar to that described for the millisecond pulsar B 1957+20 (see §4.1.1). Pulsar proper motion velocities  $v_p \gtrsim 100 \text{km s}^{-1}$  and magnetic field strength in the interstellar medium of  $B \lesssim 0.05 \text{mG}$ , comparable to the field in the Galactic center (see Morris 1994), would be required to resolve such tail-like sources given the resolution limit of the *Chandra* observations. For these parameters, we find  $\nu_c < \nu_X$ , so millisecond pulsars will have relatively higher luminosities and steeper spectra  $\Gamma \sim 2 - 2.5$  than if  $\nu_c > \nu_X$  (see §3). The photon power law index from such wind nebulae is consistent with that inferred for the observed extended sources (i.e.,  $\Gamma \sim 2$ ; see Lu, Wang, & Lang 2003). A particularly unusual source was reported by Wang, Lu, & Lang (2002) who found an elongated feature G0.13-0.11 with a high X-ray luminosity  $\sim 10^{33} \text{ergs s}^{-1}$  and long tail  $\gtrsim 10^{18}$  cm. It had been noted that a large radio filament or arc is coincident with the X-ray emission region, and Wang et al. (2002) suggested that this source is a young pulsar wind nebula. Although this interpretation is possible for such a special source, it is also possible that a millisecond pulsar interpretation is viable if the spin down power of the millisecond pulsar is the order of  $10^{35} \text{ergs s}^{-1}$  and magnetic field strengths in the surrounding medium of  $B \sim 10 \mu\text{G}$ . We note that at least four millisecond

pulsars have a spin down power equal to or larger than this level (see Becker & Aschenbach 2002). For slowly moving millisecond pulsars, the sources would appear point-like. The photon indices characterizing the spectra can lie in the range from 1.5 to 2.5 with the X-ray luminosities as high as  $10^{31} - 10^{32} \text{erg s}^{-1}$ .

Since the *Chandra* resolution limit at the Galactic center is about  $10^{17}$  cm, which is larger than the X-ray emission radius of a typical pulsar wind nebula, the X-ray emission of such sources in the *Chandra* fields should include the additional contributions from both the thermal component (due to emission from the polar cap on the neutron star surface) and non-thermal component (from the magnetosphere). Since the thermal component is soft ( $kT < 1 \text{keV}$ ) and absorbed by interstellar gas for sources at the Galactic center, only the non-thermal components associated with the processes in the neutron star magnetosphere and the pulsar wind nebula will contribute to the observed X-ray emission. We note, however, that the luminosity of the non-thermal X-rays produced as a result of synchrotron emission of electron-positron pairs in the pulsar magnetosphere is not a significant contributor to the total X-ray luminosity since the conversion efficiency is  $3 \times 10^{-4}$  (see §3). Hence, the pulsar wind nebula is likely to be the primary site of the "non-thermal" X-ray emission. On the other hand, if the observed spectrum is poorly determined, hard "thermal" X-rays emitted from the polar cap resulting from either polar cap heating of curvature radiation pairs or inverse Compton pairs (Harding & Muslimov 2002) can not be differentiated from the "non-thermal" hard X-rays.

Recently, Park et al. (2004) have pointed out the existence of a low density ( $\sim 0.1 \text{cm}^{-3}$ ), hot gaseous component in the Galactic center region. In this case the description of the pulsar wind nebula is modified from a bow shock to a termination shock picture (Cheng et al. 2004). However, the weak dependence of the X-ray luminosity on the shock radius (see equ. 3) in the fast cooling regime leads to luminosities which are not significantly different. Thus, pulsar wind nebulae from either termination or bow shocks can provide a population of faint point-like sources characterized by photon indices  $\Gamma \gtrsim 1.5$  involving non-accreting neutron stars as well as providing a potential population of faint tail-like sources complementary to the model involving fast moving knots associated with supernova remnants as discussed by Bykov (2003).

Recently, TeV  $\gamma$ -ray emission at a luminosity higher than  $10^{35} \text{ergs s}^{-1}$  from the direction of the GC has been reported by three independent groups, Whipple (Kosack et al. 2004), CANGAROO (Tsuchiya et al. 2004), and HESS (Aharonian et al. 2004). The most plausible candidates suggested for this emission include the black hole Sgr A\* (Aharonian & Neronov 2005) and the compact and powerful young supernova remnant (SNR) Sgr A East (Crocker et al. 2005). The angular scale of the TeV source was determined by

HESS to be less than a few arc-minutes, indicating that this  $\gamma$ -ray source is located in the central  $\leq 10 pc$  region (Aharonian et al. 2004). Since TeV photons are produced by inverse Compton scattering and the efficiency is not high, typically  $10^{-3} - 10^{-4}$ , it suggests that if these TeV photons are produced by PWN of MSP it requires about  $10^3$  in 10pc region even if the inverse Compton scattering efficiency is as high as 10%(Wang, et al. 2005). Such a high density of MSPs is very unlikely, and it is therefore, unlikely the PWN of MSP are responsible for TeV radiation from GC.

#### 4.2.3. Millisecond Pulsars in Globular Clusters

The contribution of pulsar wind nebulae to the X-ray emission of millisecond pulsars in globular clusters is likely to differ from that in the Galactic field. Observationally, the recent *Chandra* X-ray studies of the millisecond pulsars in 47 Tuc (Grindlay et al. 2002) reveal that these pulsars appear to be consistent with a thermal blackbody spectrum characterized by a temperature corresponding to an energy of 0.2-0.3 keV and X-ray luminosities of  $10^{30-31} \text{erg s}^{-1}$ . The emission site of this radiation is likely to be the heated polar caps on the neutron star surface with no evidence for emission from a pulsar wind nebula. On the other hand, the more recent work by Bogdanov et al. (2005) on the spectral and long-timescale variability analyses of *Chandra* observations of 18 millisecond pulsars in 47 Tuc has led to the discovery that the three sources, 47 Tuc J, O and W, exhibit a significant non-thermal component. The photon index of these three sources are in the range  $1 \pm 0.56$ ,  $1.33 \pm 0.79$ , and  $1.36 \pm 0.24$  respectively. Of these, only 47 W exhibits dramatic X-ray variability as a function of orbital phase. We note that since 47 Tuc O lies near the center of the cluster where the number density of X-ray sources is large its non-thermal spectrum may be contaminated by background sources in the field. Of the remaining two millisecond pulsars, it is possible that the non-thermal spectral components are produced in an intrabinary shock formed by the interaction between the relativistic wind and matter from the stellar companion (Bogdanov et al. 2005). Thus, these observations do not suggest a magnetospheric origin for the non thermal emission at such levels. The much higher non-thermal X-ray luminosity from W ( $\sim 2.7 \times 10^{31} \text{ ergs s}^{-1}$ ), in comparison to J ( $\sim 9.3 \times 10^{30} \text{ ergs s}^{-1}$ ), may reflect the differing nature of the companion star. A main sequence companion star nearly filling its Roche lobe and of mass  $\gtrsim 0.13 M_{\odot}$  is associated with W whereas a brown dwarf underfilling its Roche lobe and of mass  $\lesssim 0.03 M_{\odot}$  is associated with J. The X-ray luminosity of the non-thermal components from these MSPs can be estimated following the discussion given in §3.3. Taking an average spin-down power of the millisecond pulsars in 47 Tuc,  $\dot{E} \sim 2 \times 10^{34} \text{ erg s}^{-1}$ ,  $p = 2.3$ ,  $\epsilon_B \sim 0.003$ ,  $\epsilon_e \sim 0.5$ ,  $\gamma_w \sim 10^6$ , and  $\Omega = 1$ , we find an non-thermal X-ray luminosity

in the band 0.1-10 keV of  $4 \times 10^{29} \text{erg s}^{-1}$  for an assumed  $R_s \sim 10^{11} \text{cm}$ . If we choose  $\epsilon_B \sim 0.1, \gamma_w \sim 2 \times 10^5$ , a larger X-ray luminosity  $\sim 4 \times 10^{30} \text{erg s}^{-1}$  results, which is closer to the observed values. This may suggest that  $\epsilon_B$  in PWN of MSPs is indeed larger. The remaining deviation by a factor of 3 may suggest an underestimate of the spin down power of these millisecond pulsars by a factor of  $\sim 2$ .

Pulsar wind nebulae are not likely to significantly contribute to the non-thermal emission from millisecond pulsars in 47 Tuc since the nebula is significantly affected by its interaction with cluster stars. An estimate of the bow shock radius follows from equ (1). Here, we adopt an electron density of  $\sim 0.1 \text{cm}^{-3}$  as inferred from the electron dispersion measures from the radio pulses (Freire et al. 2001). Since the millisecond pulsars lie in the core of the cluster, we assume that the pulsar's mean velocity is  $\sim 10 \text{km s}^{-1}$ . Taking the mean spin-down power of the pulsars to be  $\dot{E} \sim 2 \times 10^{34} \text{erg s}^{-1}$  (Cheng & Taam 2003), leads to a termination radius of the pulsar wind nebula in the case of a bow shock of  $R_s \sim 2 \times 10^{18} \text{cm}$ . This length scale is significantly larger than the average distance between stars ( $\lesssim 10^{17} \text{cm}$ ) within three core radii of 47 Tuc where millisecond pulsars are primarily found in the cluster. Hence, the interaction of stars with the nebula is likely to significantly diminish any non-thermal non-pulsed X-ray emission associated with this diffuse region.

This result is also expected to apply to PSR B1821-24, the brightest millisecond pulsar in the Galaxy. PSR B1821-24 was the first millisecond pulsar to be discovered in a globular cluster (Lyne et al. 1987), having been found in M28. It is characterized by a pulse period of 3.05 ms and a spin down power of  $2.2 \times 10^{36} \text{ergs s}^{-1}$ . In contrast to the isolated millisecond pulsars in 47 Tuc, its spectrum is apparently non-thermal with a power law index  $\Gamma = 1.2_{-0.13}^{+0.15}$  (see Becker et al. 2003). In addition, the X-ray luminosity of the diffuse component of B1821-24 is somewhat uncertain because of source confusion as it is located in the core of M28. In particular, Becker et al. (2003) obtained *Chandra*/ACIS-S spectral observations of the field of M28 and found 46 point sources above a limiting luminosity of  $6 \times 10^{30} \text{erg s}^{-1}$ . On the other hand, Rutledge et al. (2004), using the *Chandra*/HRC-S instrument to perform absolute timing observations of B1821-24, found 7 sources including B1821-24 within the  $14''.4$  core radius of M28. The time averaged X-ray luminosity was found by Rutledge et al. (2004) to be  $(4.0 \pm 0.2) \times 10^{32} \text{ergs s}^{-1}$  (0.1-2.0KeV) of which 15% (or  $6 \times 10^{31} \text{ergs s}^{-1}$ ) was attributed to the nonpulsed component. Although the spectrum of this component is not known, its luminosity level corresponds to a very small fraction ( $\sim 3 \times 10^{-5}$ ) of the spin down power of B1821-24 and could originate from source confusion or from some residual nearly isotropic magnetospheric X-ray emission.

Based on the interpretation for the lack of non-thermal emission for the isolated millisecond pulsars in 47 Tuc, it is likely that stellar interactions with the relativistic

wind from B1821-24 would significantly affect the establishment of a PWN. Specifically, the termination shock radius is estimated to be of the order of 1 pc, while the high core density in M28 ( $\sim 10^5$  stars  $\text{pc}^{-3}$ ) indicates that the average distance between stars is 50 times smaller. Hence, the results described above suggest that the low level of non-thermal non-pulsed X-ray emission from PSR B1821-24 may represent the contribution from the pulsar’s magnetosphere.

## 5. DISCUSSION

For the 8 millisecond pulsars in the Galactic field for which the 2-10 keV total X-ray luminosity can be determined, 2 have been published with the pulsed and non-pulsed emission components. In this paper, we have interpreted the non-pulsed component as arising from a PWN. Evidence in support of such an interpretation is provided by the observation of diffuse X-ray emission in the millisecond pulsar, B1957+20 (Stappers et al. 2003). For the majority of millisecond pulsars where X-ray emission has been detected (see Table 1), the X-ray emission is not spatially resolved. Since the X-ray luminosity associated with the pulsed emission from the pulsar’s magnetosphere is expected to be a relatively small fraction of the total X-ray luminosity,  $L_X^{\text{pul}}/\dot{E} \sim 3 \times 10^{-4}$  in the model of Cheng et al. (1998) and Zhang & Cheng (2003), it is likely that the wind nebulae significantly contribute to the observed X-ray radiation.

A simple one-zone model for the X-ray emission from the nebula (Cheng, Taam & Wang 2004), based on the work of Chevalier (2000), indicates that the efficiency for the conversion of rotational energy of the neutron star to X-ray emission can be significantly higher in the post shocked region of the wind nebula than in the neutron star magnetosphere. In this model, the X-ray luminosities primarily depend upon the spin down power of the pulsar and particle and magnetic field energy densities behind the shock and only weakly dependent on the pulsar’s velocity and the number density of the surrounding interstellar medium. The X-ray emission is characteristically non-thermal and described by a power law with photon index lying in the range between 1.5 and 2.5, with the efficiency of conversion of spin down power to X-ray luminosity greater in the fast cooling regime (where  $\Gamma \sim 2 - 2.5$ ) than in the slow cooling regime (where  $\Gamma \sim 1.5 - 2$ ). In our interpretation, the X-ray source may be either point-like or tail-like in appearance, and we interpret the elongated tail observed in several faint X-ray sources as the distance traversed by the pulsar within the synchrotron emission cooling timescale. Pulsars moving more rapidly than  $100 \text{ km s}^{-1}$  in regions of the interstellar medium characterized by magnetic field strengths  $\lesssim 0.1 \text{ mG}$  are likely to exhibit a tail-like structure even at distances comparable to the Galactic center. For example,

for  $B \sim 0.03$  mG and  $v_p \sim 150$  km s<sup>-1</sup> the tail can extend to  $\sim 3 \times 10^{17}$  cm, a length scale comparable to that of elongated sources observed in the deep *Chandra* surveys of the Galactic center (see Wang et al. 2002b, Munro et al. 2003). The majority of the sources, on the other hand, are likely to have much smaller sized nebulae, making them appear point-like. For typical spin parameters of millisecond pulsars, the X-ray luminosity level can be as high as  $\sim 10^{31} - 10^{32}$  ergs s<sup>-1</sup>, perhaps making them an important contributor to the faint X-ray source population associated with neutron stars in deep X-ray surveys.

Because the emission from PWN is spatially extended and can exceed the luminosity of the neutron star, the measured emission from a pulsar may be a function of the size of the region studied. As the size depends on the magnetic field and number density of the pulsar’s environment, we illustrate their range by listing in Table 2 the estimated size of the pulsar wind nebulae surrounding millisecond pulsars, for physical conditions in the Galactic center and in B1957+20. For comparison, the highest spatial resolution afforded by the *Chandra* observations is also listed showing that the PWN can be entirely contained within or extend beyond the aperture radius respectively. Although the simple one-zone model is inadequate to predict the spatial variation of the photon power law index and luminosity, it is expected that the X-ray properties of pulsars surrounded by wind nebulae are likely to be a function of the observed spatial resolution.

We have suggested that the contribution of the PWN to the non-pulsed non thermal emission of millisecond pulsars in the cores of globular clusters is likely reduced due to the effect of interaction of stars with it. Hence, the non-thermal X-ray contribution due to the PWN to the total X-ray emission may not be important in comparison to millisecond pulsars in the Galactic field. For those millisecond pulsars with a binary companion in globular cluster systems, the emission from an intrabinary shock can be an important contributor to the non-thermal non-pulsed X-ray emission. In particular, it has been found (see equation 7) that the non-thermal X-ray emission from an intrabinary shock in a binary millisecond pulsar system is very sensitive to the spin down power. For example, a spin down power of  $10^{34}$  ergs s<sup>-1</sup> would yield a non-thermal X-ray luminosity of  $\sim 3 \times 10^{29}$  erg s<sup>-1</sup> for  $p = 2.2$ , making them difficult to detect at the present time. Thus, the lack of non-thermal X-ray emission from the majority of binary millisecond pulsars in 47 Tuc suggests that  $\dot{E} \lesssim 10^{34}$  ergs s<sup>-1</sup> for the majority of these binary millisecond pulsars.

In contrast, the non-thermal emission from isolated millisecond pulsars in globular clusters may have a contribution from the magnetosphere. The identification of a non-thermal non-pulsed component in globular cluster millisecond pulsars uncontaminated by source confusion could be especially important in constraining the flux level of such a component in pulsar emission models. Some unpulsed X-ray emission is expected if the

distribution of the pitch angles of charged particles in the magnetosphere is uniform. In this case, the synchrotron radiation from particles with very large pitch angle, say larger than  $80^\circ$ , will tend to radiate isotropically. The luminosity of this component can be estimated as  $L_x(\text{unpulsed})/\dot{E} = (L_x(\text{unpulsed})/L_x(\text{pulsed}))(L_x(\text{pulsed})/\dot{E}) \sim \cos(80^\circ)3 \times 10^{-4} \sim 5 \times 10^{-5}$ . Here we have assumed that  $(L_x(\text{unpulsed})/L_x(\text{pulsed}))$  is given by the ratio of their angular distribution  $\sim \cos(80^\circ)$  and  $(L_x(\text{pulsed})/\dot{E}) \sim 3 \times 10^{-4}$  is estimated by Cheng & Zhang (1999). Such a level of emission is comparable to the off-pulse X-ray emission detected from PSR J0218+4232 and PSR B1821-24 (e.g. Mineo et al. 2000). We remark that other emission sites for non-thermal non-pulsed X-rays have been suggested. For example, Cheung & Cheng (1994) have argued that pair production can still continue beyond the light cylinder, where the magnetic field lines are twisted and the pitch angles of the created pairs are large. Consequently the radiation of relativistic electron and positron pairs will be not beamed. The characteristic photon index is  $\sim 1.5$ . Without high angular resolution, it will be difficult to distinguish the origin of the non-pulsed non-thermal X-ray emission. In particular, the photon index of the X-ray emission from the shock region in the slow cooling regime cannot be differentiated from the unpulsed emission originating in the magnetosphere, making direct observational determination of the non-thermal X-ray emission location challenging.

Our model X-ray luminosity depends on several shock parameters. In particular,  $\epsilon_B$  and  $\gamma_w$  are poorly determined. However, both equation 3 and equation 5 do not sensitively depend on  $\gamma_w$  if  $p$  is around 2. Again the dependence on  $\epsilon_B$  in equation 3 is also very weak. However, this parameter become important for the case of an intrabinary shock. In fact, by comparing with systems with a contribution from an intrabinary shock the inferred  $\epsilon_B$  is significant larger than that of the Crab nebula. For example,  $\epsilon_B \sim 0.02$  can match the observed data of PSR1957+20. Although this is significantly higher than inferred for the Crab nebula, it is consistent with the value obtained in PSR 1259-63 (Tavani & Arons 1997). These results taken together point to the importance of the environmental properties of the surrounding medium on estimates of  $\epsilon_B$ .

In this paper, we have further assumed that  $B_d \cdot \Omega < 0$  in estimating the potential drop, where  $B_d$  and  $\Omega$  are the dipole magnetic field and the angular velocity of the star respectively. In the case of  $B_d \cdot \Omega > 0$ , Harding, Usov & Muslimov (2005) showed that the potential drop in the polar gap could be much larger than that estimated in §3.1, however, the X-ray emission associated with the polar gap emission will be pulsed and also correlated with the gamma-ray emission. Therefore this may provide a test to discriminate these two cases.

Finally, the pulsar wind interacting with a companion star and/or the interstellar

medium may also contribute to the hard X-ray emission associated with soft X-ray transients in quiescence if a millisecond pulsar is activated during temporary states when the accretion of mass is significantly reduced or prevented by a rapidly rotating magnetosphere (Illarionov & Sunyaev 1975). We suggest that observations be carried out to search for the non-thermal radio emission that would accompany the hard X-ray emission associated with the synchrotron radiation process to confirm the viability of such an interpretation. If detected, millisecond pulsars in isolation and in binary systems may be more important contributors to the faint X-ray source population in the Galaxy than has hitherto been considered. Such an association may prove useful as a means of identifying candidate objects for further radio pulse timing searches of new millisecond pulsars.

We are grateful for useful comments from the referee and discussions with Drs. Craig Heinke and Werner Becker. This work is partially supported by the NSF through grant AST-0200876, by a RGC grant of the Hong Kong Government, by the National Natural Science Foundation of China under grant 10273011 and by the Theoretical Institute of Advanced Research in Astrophysics (TIARA) in Taiwan.

## REFERENCES

- Aharonian, F.A., et al. 2004, *A&A*, 425, L13
- Aharonian, F.A., & Neronov, A., 2005, *ApJ*, 619, 306
- Alpar M.A., Cheng A.F., Ruderman M.A., Shaham J., 1982, *Nat*, 300, 728
- Arons, J. 1981, *ApJ*, 284, 1099
- Arons, J. & Tavani, M., 1993, *ApJ*, 403, 249
- Arzoumanian, A., Fruchter, A. S., & Taylor, J. H., 1994, *ApJ*, 426, L85
- Backer, D. C., Kulkarni, S. R., Heiles, C., Davis, M. M., & Goss, W. M. 1982, *Nature*, 300, 615
- Bailes, M. et al. 1997, *ApJ*, 481, 386
- Beck, R., Shukurov, A., Sokoloff, D., Wielebinski, R. 2003, *A&A*, 411, 99
- Becker, W. & Aschenbach, B. 2002, “Neutron Stars, Pulsars and Supernova Remnants” eds. W. Becker, H. Lesch & J. Trümper, MPE Report 278, 64
- Becker, W. & Trümper, J. 1993, *Nature*, 365, 528
- Becker, W. & Trümper, J. 1997, *A&A*, 326, 682

- Becker, W. & Trümper, J. 1998, IAU circular 6829
- Becker, W. & Trümper, J. 1999, A&A, 341, 803
- Becker, W. et al. 2003, ApJ, 594, 798
- Becker, W. et al. 2005, ApJ, submitted
- Bednarz, J. & Ostrowski, M. 1998, Phys. Rev. Lett., 80, 3911
- Belczynski, K., & Taam, R. E. 2004, ApJ, 616, 1159
- Blondin, J.M., Chevalier, R.A. & Frierson, D.M. 2001, ApJ, 563, 806
- Bogdanov, S., Grindlay, J. E., & van den Berg M. 2005, ApJ, 630, 1029
- Bogdanov, S., Grindlay, J. E., Heinke, C., Camilo, F. Freire, P. C. , Becker, W. 2005, submitted to ApJ
- Bykov, A. M. 2003, A&A, 410, L5
- Bucciantini, N. 2002, A&A, 387, 1066
- Campana, S., Colpi, M., Mereghetti, S., Stella, L., & Tavani, M. 1998, A&A Rev., 8. 279
- Campana, S. et al. 2004, ApJ, 614, L49
- Campana, S., & Stella, L. 2003, astro-ph/0309811
- Cheng, A. F., & Ruderman, M. A. 1980, ApJ, 235, 576
- Cheng, K. S., Gil, J. & Zhang, L. 1998, ApJ, 493, L35
- Cheng, K. S., & Taam, R.E. 2003, ApJ, 598, 1207
- Cheng, K. S., Taam, R. E., and Wang, W. 2004, ApJ, 617, 480
- Cheng, K. S. & Zhang, L. 1999, ApJ, 515, 337
- Cheung, W.M., & Cheng, K. S. 1994, ApJS, 90, 827
- Chevalier, R. A. 2000, ApJ, 539, L45
- Cordes, J.M. & Lazio, T.J.W. 2002, astro-ph/0207156
- Crocker, R.M., et al., 2005, ApJ, 622, 892
- de Jager, O.C. & Harding, A.K. 1992, ApJ, 396, 161
- Freire, P. C. et al. 2001, ApJ, 557, L105
- Fruchter, A. S., Stinebring, D. R., & Taylor, J. H. 1988, Nature, 333, 23
- Gaensler, B.M. 2004, in IAU Symposium 218 "Young Neutron Stars and Their Environments" eds F. Camilo & B.M. Gaensler (astro-ph/0405290)
- Goldreich, P., & Julian, W.H. 1969, ApJ, 157, 859

- Grindlay, J. E. et al. 2002, *ApJ*, 581, 470
- Harding, A. K., & Muslimov, A.G. 2001, *ApJ*, 556, 987
- Harding, A. K., & Muslimov, A.G. 2002, *ApJ*, 568, 862
- Harding, A. K., Usov, V.V., & Muslimov, A.G. 2005, *ApJ*, 622, 531
- Helfand, D. J., Gotthelf, E. V., & Halpern, J. P. 2001, *ApJ*, 556, 380
- Hui, C.Y. & Becker, W. 2005, *A&A*, submitted for publication
- Illarionov, A., & Sunyaev, R. 1975, *A&A*, 39, 185
- in 't Zand, J. J. M. et al. 2001, *A&A*, 372, 916
- Jonker, P. G., Wijnands, R., & van der Klis 2004, *MNRAS*, 349, 94
- Jones, P. 1980, *MNRAS*, 192, 847
- Kennel, C. F. & Coroniti, F. V. 1984, *ApJ*, 283, 694
- Komissarov, S.S. & Lyubarksi, Y.E. 2003, *MNRAS*, 344, L93
- Kosack, K. et al., 2004, *ApJ*, 608, L97
- Kulkarni, S. R., & Hester, J. J. 1988, *Nature*, 335, 801
- Lemoine, M. & Pelletier, G. 2003, *ApJ*, 589, L73
- Lu, F. Wang, Q.D. & Lang, C. 2003, *AJ*, 126, 319
- Lyne, A. G., Brinklow, A., Middleditch, J., Kulkarni, S. R., Backer, D. C., & Clifton, T. R. 1987, *Nature*, 328, 399
- Lyne, A. G., Manchester, R. N., Lorimer, D. R., Bailes, M., D'Amico, N., Tauris, T. M., Johnston, S., Bell, J. F., & Nicastro, L. 1998, *MNRAS*, 295, 743
- Mineo, T. et al. 2000, *A&A*, 355, 1053
- Morris, M. 1994, *The Nuclei of Galaxies*, eds. Reinhard Genzel & Andres I. Harris (Kluwer, Dordrecht), p. 185
- Muno, M. P., et al. 2003, *ApJ*, 589, 225
- Muno, M. P., et al. 2004, *ApJ*, 613, 1179
- Nicastro, L. et al. 2004, *A&A*, 413, 1065
- Ögelman, H. 1995, in *The Lives of Neutron Stars*, eds. A. Alpar, U. Kilizoglu & J. van Paradijs, (Kluwer, Dordrecht), p. 101
- Park, S., Muno, M. P., Baganoff, F. K., Maeda, Y., Morris, M., Howard, C., Bautz, M. W., & Garmire, G. P. 2004, *ApJ*, 603, 548

- Peterson, L. E. & Jacobson, A. S. 1970, *PASP*, 82, 412
- Phinney, E. S., & Kulkarni, S. R. 1994, *ARA&A*, 32, 591
- Psaltis, D., & Chakrabarty, D. 1999, *ApJ*, 521, 332
- Ruderman, M., Shaham, J. & Tavani, M., 1989, *ApJ*, 336, 507
- Rutledge, R. E., Fox, D. W., Kulkarni, S. R., Jacoby, B. A., Cognard, I., Backer, D. C., & Murray, S. S. 2004, *ApJ*, 613, 522
- Sakurai, I. et al. 2001, *PASJ*, 53, 535
- Saito, Y. et al. 1997b, *ApJ*, 477, L37
- Saito, Y. 1998, Ph.D. Thesis, Univ. of Tokyo
- Sefako, R.R. & DeJager, O.C. 2003, *ApJ*, 593, 1013
- Seward, F. D., & Wang, Z. R. 1988, *ApJ*, 332, 199
- Stappers, B. W., Gaensler, B. M., Kaspi, V. M., van der Klis, M., & Lewin, W. H. G. 2003, *Science*, 299, 1372
- Stella, L. et al. 1994, *ApJ*, 423, L47
- Tavani, M., Arons, J. & Kaspi, V. M. 1994, 433, L37
- Tavani, M. & Arons, J. 1997, 477, 439
- Toscano, M. et al. 1999, *MNRAS*, 307, 925
- Tsuchiya, K. et al. 2004, *ApJ*, 606, L115
- Tsuruta, S. 1998, *Phy. Rep.*, 292 1
- van der Swaluw, E. *A&A*, 404, 939
- Wang, Q.D., Gotthelf, E.V., & Lang, C.C. 2002, *Nature*, 415, 148
- Wang, Q.D., Lu, F. & Lang, C. 2002, *ApJ*, 581, 1148
- Wang, W., Jiang, Z.J., Pun, J.C.S. & Cheng, K.S. 2005, *MNRAS*, 360, 646
- Webb, N. A., Olive, J.-F & Barret, D. 2004a, *A&A*, 417, 181
- Webb, N. A., Olive, J.-F, Barret, D., Kramer, M., Cognard, I. & Löhmer, O., 2004b, *A&A*, 419, 269
- Weisskopf M. C. et al. 2000, *ApJ*, 536, L81
- Wijnands, R., & van der Klis, M. 1998, *Nature*, 394, 344
- Zavlin, V.E. et al., 2002, *ApJ*, 569, 894
- Zhang, B., & Harding, A. K. 2000, *ApJ*, 532, 1150

Zhang, L. & Cheng, K.S. 2003, A&A, 398, 639

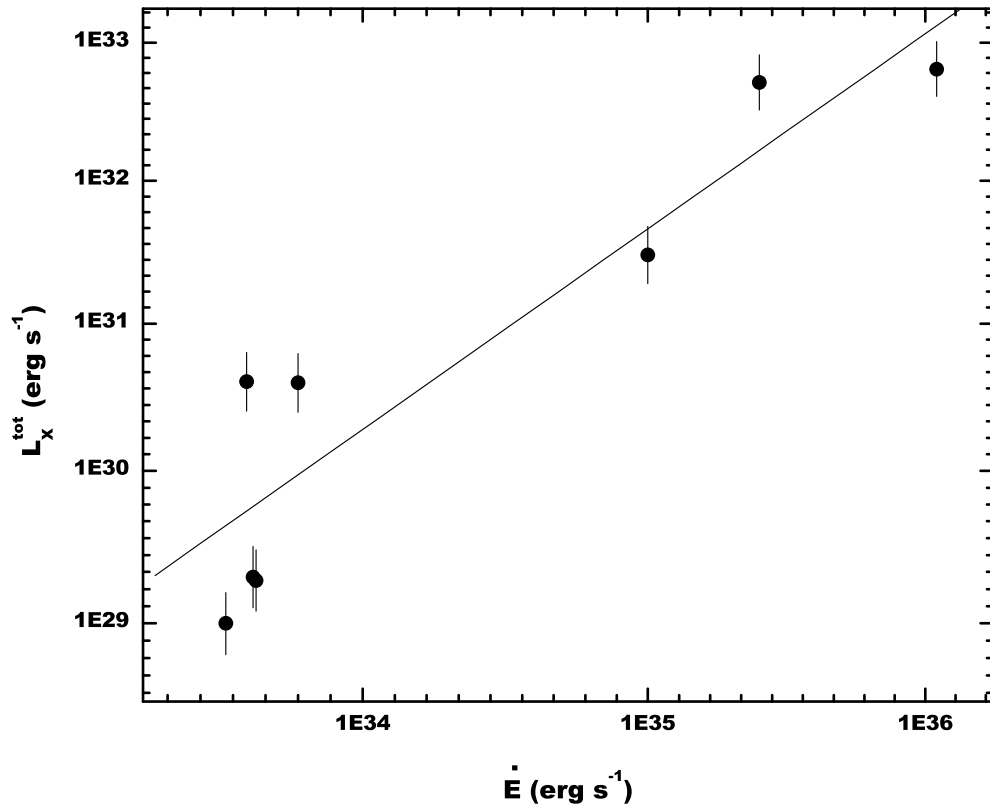


Fig. 1.— The total X-ray luminosity (2-10 keV) versus spin-down power of 8 millisecond pulsars. The solid line is the best fitting with a function with  $L_x \propto \dot{E}^{1.39 \pm 0.08} \text{ ergs s}^{-1}$ .

Table 1: X-ray properties of some millisecond pulsars

PSR	$P$ (ms)	$\dot{P}$ (s s <sup>-1</sup> )	$d$	$\dot{E}$	$L_{X,tot}$	$L_{X,pul}$	$L_{X,npul}$	$\Gamma$	Reference
B1937+21	1.56	$1.05 \times 10^{-19}$	3.6	$1.1 \times 10^{36}$	$6.4 \times 10^{32}$	$4.6 \times 10^{32}$	$1.8 \times 10^{31}$	$\frac{1.21 \pm 0.15^a}{3.3 \pm 0.5^b}$	1
J2124-3358	4.93	$1.3 \times 10^{-20}$	0.25	$4.3 \times 10^{33}$	$1.9 \times 10^{29}$			$2.8 \pm 0.6^d$	2
J0437-47	5.8	$1.9 \times 10^{-20}$	0.139 <sup>c</sup>	$4.2 \times 10^{33}$	$2.0 \times 10^{29}$			$2.2 \pm 0.3$	3
J0030+0451	4.87	$1.0 \times 10^{-20}$	0.23	$3.4 \times 10^{33}$	$1.0 \times 10^{29}$			$3 \pm 0.4$	4
J0218+4232	2.3	$7.5 \times 10^{-20}$	2.7 <sup>c</sup>	$2.5 \times 10^{35}$	$5.12 \times 10^{32}$	$4.6 \times 10^{32}$	$3 \times 10^{31}$	$\frac{0.61 \pm 0.32^a}{1.17 \pm 0.37^b}$	5, 6
J0751+1807	3.48	$8 \times 10^{-21}$	1.1 <sup>c</sup>	$6 \times 10^{33}$	$3.93 \times 10^{30}$			$1.59 \pm 0.2$	7
J1012+5307	5.3	$1.5 \times 10^{-20}$	0.77 <sup>c</sup>	$4 \times 10^{33}$	$4.0 \times 10^{30}$			$1.78 \pm 0.36$	7
B1957+20	1.6	$1 \times 10^{-20}$	2.5 <sup>c</sup>	$1 \times 10^{35}$	$3.0 \times 10^{31}$			$1.9 \pm 0.5$	7

Note. — The first column PSR is the pulsar name,  $P$  is the spin period,  $\dot{P}$  is the period derivative,  $d$  is the distance of the pulsar in units of kpc. The luminosity is in units of erg s<sup>-1</sup>.  $\dot{E}$  is the pulsar’s spin-down power.  $L_{X,tot}$  is the total X-ray luminosity,  $L_{X,pul}$  is just the pulsed X-ray luminosity,  $L_{X,npul}$  is the non pulsed luminosity. In calculating the pulsed X-ray luminosity, the solid angle is assumed to be unity.  $\Gamma$  is the photon index. The luminosities are taken from the observations of *ASCA*, *BeppoSAX*, *XMM-Newton* and *Chandra* in the energy range of 2-10 keV. We have approximated errors in  $\log(L_x)$  as  $\pm 0.2$ .

<sup>a</sup>  $\Gamma$  of the pulsed components ;

<sup>b</sup>  $\Gamma$  of the nonpulsed components;

<sup>c</sup> Accurate distance estimates (Bogdanov et al. 2005). Other estimates are obtained mainly from dispersion measure together with the Cordes & Lazio (2002) electron density model and are rather uncertain.

<sup>d</sup>  $\Gamma = 2.2 \pm 0.3$  given by Hui & Becker (2005) Reference: 1. Nicastro et al. 2004; 2. Sakurai et al. 2001; 3. Zavlin et al. 2002; 4. Becker & Aschenbach 2002; 5. Mineo et al. 2000; 6. Webb et al. 2004a; 7. Webb et al. 2004b; 8. Stappers et al. 2003

Table 2: Relative size of pulsar wind nebulae with respect to Chandra resolution for millisecond pulsars in two different environments

	$D$ (kpc)	$n$ ( $\text{cm}^{-3}$ )	$B$ G	$v_p^\dagger$ ( $\text{km s}^{-1}$ )	$\delta\theta$	$R_{\text{obs}}$ (cm)	$R_s$ (cm)
GC	8.5	$10^2$	$10^{-4}$	130	1''	$6 \times 10^{16}$	$2 \times 10^{15}$
1957+20	1.5	1	$10^{-5}$	220	1''	$1 \times 10^{16}$	$4 \times 10^{16}$

---

Note. — Millisecond pulsars in the Galactic Center and PSR B1957+20.  $D$  is the distance,  $n$  is the number density in the medium surrounding the pulsar,  $B$  is the magnetic field in the interstellar medium,  $v_p$  is the pulsar proper motion velocity,  $\delta\theta$  is the detection angular limit in the different observations,  $R_{\text{obs}} \sim D\delta\theta/2$  is the radius of the aperture, and  $R_s$  is the predicted shock radius.

<sup>†</sup> For the Galactic center, we take a spin down power of  $2 \times 10^{34}$  ergs  $\text{s}^{-1}$  and an average velocity of pulsars of  $130 \text{ km s}^{-1}$ , which is lower than the escape speed from this region.